Time-Dependent FEM Modeling for Transcutaneous Oxygen Sensors

Mohammed Almatrood[1] and Bige D. Unluturk[2]

***Abstract*— Continuous, real-time respiratory monitoring is essential in managing chronic respiratory diseases, perioperative care, and critical care settings, where the rapid and accurate detection of hypoxia can significantly impact ~~patient~~ patients' outcomes. Transcutaneous oxygen monitoring ($PtcO_2$) is an emerging wearable sensing technology that measures the partial pressure of oxygen diffusing through the skin ~~,~~ which correlates with arterial oxygen partial pressure (PaO_2), ~~which is~~ the clinical gold standard. Despite its promise, the clinical adoption of $PtcO_2$ has been limited. Prior studies have primarily focused on direct comparisons between PaO_2 and $PtcO_2$, yielding mixed results regarding their agreement and limiting $PtcO_2$ to trend monitoring. To address this gap, we propose a finite element modeling (FEM) framework to investigate the physiological relationship between PaO_2 and $PtcO_2$. By simulating oxygen transport across multiple skin layers, the model provides mechanistic insights into transcutaneous oxygen dynamics under varying physiological conditions, such as arterial oxygen fluctuations and localized blood flow occlusion. This personalized computational model aims to improve the accuracy and reliability of transcutaneous oxygen monitoring, enabling more effective continuous respiratory assessment.**

I. INTRODUCTION

Accurate, real-time quantification of arterial oxygen partial pressure (PaO_2) is essential for effective management of various respiratory disorders, including chronic obstructive pulmonary disease (COPD) and asthma, among others. Clinical methods such as arterial blood gas analysis (ABG) and pulse oximetry are commonly used; however, both methods present significant limitations. For instance, ABG, while providing detailed and accurate insights into blood gas content, remains invasive, painful, and impractical for continuous monitoring, as it provides only a snapshot of a rapidly changing parameter [1]. ~~On the other hand, although~~ Noninvasive method of pulse oximetry is widely used~~due to its non-invasive nature, ~~, but it measures only oxygen saturation ~~levels~~ (SpO_2) and is influenced by peripheral perfusion, ambient light conditions, skin pigmentation, leading to potential inaccuracies [2], [3].

Transcutaneous oxygen partial pressure ($PtcO_2$) monitoring is a promising method for continuous, non-invasive, real-time assessment. Luminescence-based wearable sensors have recently emerged as cost-effective tools for $PtcO_2$ measurement [4]. However, these devices face challenges stemming from physiological variability, which limits the reliability of $PtcO_2$ as a surrogate of PaO_2 [5], [6].

[1]Mohammed Almatrood is with the Institute for Quantitative Health Science and Engineering, Department of Biomedical Engineering, Michigan State University, East Lansing, MI, USA, almatro2@msu.edu

[2]Bige D. Unluturk is with the Institute for Quantitative Health Science and Engineering, Departments of Electrical & Computer Engineering, and Biomedical Engineering, Michigan State University, East Lansing, MI, USA, unluturk@msu.edu

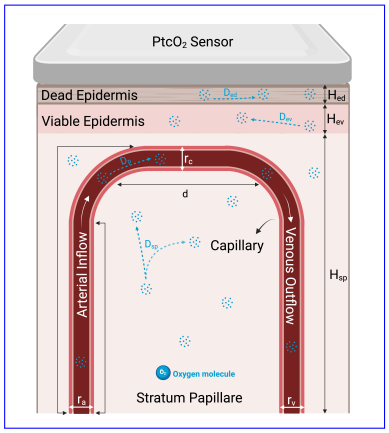

Fig. 1: Cross-section of skin microcirculatory unit ~~used in our model~~ [7].

To overcome these limitations, this paper proposes a computational framework based on finite element modeling (FEM). We develop a ~~three-dimensional~~ 3D multilayer skin model and simulate the transport of oxygen through it~~based on convection-diffusion-reaction equations~~. We incorporate adjustable parameters~~like~~ , such as skin thickness and oxygen consumption, to reflect individual variability, enabling more accurate and personalized transcutaneous oxygen monitoring.

II. RELATED WORK

Commercial transcutaneous oxygen monitoring devices use heating to enhance oxygen diffusion through the skin, considering that this allows $PtcO_2$ to approximate PaO_2. However, excessive heating can alter the local blood flow and cause vascular changes that may not reflect systemic oxygenation [8], while insufficient heating can lead to underestimation of tissue oxygen levels [9]. Heating also poses risks of skin burns and irritation, particularly in sensitive populations like neonates [10].

To address these limitations, a new ~~luminescence based transcutaenous~~ luminescence-based transcutaneous sensing technology was developed that eliminates the use of heating elements [11]. However, this approach can potentially widen the discrepancy between PaO_2 and $PtcO_2$. To ~~bridge this gap~~estimate PaO_2 from $PtcO_2$ even for the non-heating sensors, we aim to develop a model describing the relationship of $PtcO_2$ and PaO_2.

Oxygen transport in skin was first modeled by Krogh whose model describes radial oxygen diffusion from a capillary into surrounding tissue, assuming steady-state conditions and uniform consumption [12]. While foundational, it oversimplifies skin structure. Another approach by Grossman ~~build~~ built a model based on multilayered skin structure

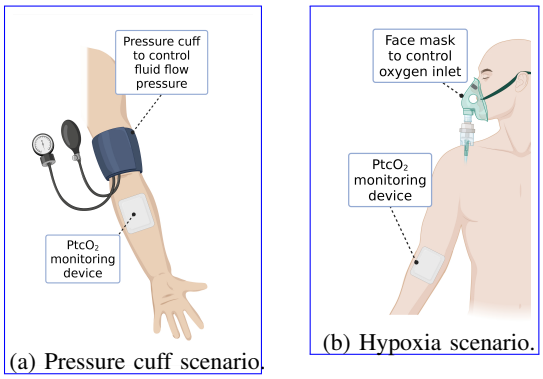

(a) Pressure cuff scenario. (b) Hypoxia scenario.

Fig. 2: Human tests scenarios used in FEM studies [14].

and accounting for differences in diffusion coefficients and metabolic activity across layers [13].

III. Methods

To investigate the relationship between $PtcO_2$ and PaO_2, we developed a partial differential equation (PDE)-based oxygen transport model within a 3D multilayer skin structure inspired by Grossmann's model (Fig. 1). ~~Finite Element Modeling (FEM)~~ FEM was then performed in COMSOL Multiphysics to simulate oxygen transport based on this model. We focused on time-dependent behavior to replicate the experimental conditions in [11], where $PtcO_2$ is measured under modulated ~~PacO~~PaO_2 using either local occlusion with blood pressure cuff or systemic hypoxia via hypoxia mask as shown in Fig. 2.

A. Grossmann's Model

The model ~~characterizes~~ describes oxygen dynamics within each layer:

- **Dead epidermis (ed, outer non-viable part of skin):** Oxygen transport is governed solely by diffusion, with no metabolic oxygen consumption.
- **Viable epidermis (ev, inner metabolically active region):** Transport of oxygen is diffusive, but with a constant rate of oxygen consumption.
- **Stratum papillare (sp, vascularized dermal layer beneath the epidermis):** This layer contains capillaries, and ~~thus~~ oxygen transport occurs via both diffusion and convection. Diffusion-driven transport with steady oxygen consumption is assumed within the surrounding ~~connective~~ tissue.

1) Oxygen Transport Equations: A set of ~~partial differential equations~~ PDEs was used to describe the blood flow and oxygen transport inside the capillaries and across each skin layer as follows

- Capillary (c) (diffusion and convection):

$$0 = \nabla \cdot \left(\alpha_{\text{cap}c} D_{\text{cap}c} \nabla P - V \left[\alpha_{\text{cap}c} P + H C_{\text{Hb}} S_0(P) \right] \right) \tag{1}$$

- Viable epidermis (ev) and stratum papillare (sp) (diffusion with consumption):

$$0 = \nabla \cdot (\alpha_i D_i \nabla P) - A(P), \quad i = \text{sp, ev} \tag{2}$$

- Dead epidermis (ed) (diffusion only):

$$0 = \nabla \cdot (\alpha_{\text{ed}} D_{\text{ed}} \nabla P) \tag{3}$$

Here, P denotes the oxygen partial pressure (kPa), α is the oxygen solubility coefficient (ml O_2/g-kPa), V is the velocity field (cm/s), C_{Hb} is the hemoglobin concentration (gHb/gblood), H is the Hüfner number (ml O_2/gHb), and $S_0(P)$ represents the oxygen-hemoglobin dissociation curve.

The oxygen dissociation curve is defined as

$$S_0(P) = \frac{1}{4} \sum_{i=1}^{4} \frac{i \cdot a_i \cdot P^i}{1 + \sum_{i=1}^{4} a_i \cdot P^i} \tag{4}$$

where a_i are the dissociation constants.

2) Fluid Flow Equations: The laminar flow of blood within the capillary is modeled using the incompressible Navier-Stokes equations

$$\rho \frac{\partial \mathbf{u}}{\partial t} + \rho(\mathbf{u} \cdot \nabla)\mathbf{u} = \nabla \cdot [-P \cdot \mathbf{I} + \mathbf{K}] + \mathbf{F}, \quad \mathbf{K} = \mu(\nabla \mathbf{u} + (\nabla \mathbf{u})^T) \tag{5}$$

where ρ is the fluid density (kg/m^3), μ is the dynamic viscosity (Pa·s), $\mathbf{F}$ is the body force (N/m^3), and $\mathbf{I}$ is the identity matrix.

3) Boundary Conditions: The only boundary conditions considered at the skin surface ~~was No-flux~~were no-flux, assuming the sensor ~~lays~~ lies on top of the skin unit ~~,~~ perfectly adhered, and effectively blocking oxygen exchange with the air, which can be ~~described mathematically as $\frac{\partial P}{\partial n} = 0$.~~ expressed as $\frac{\partial P}{\partial n} = 0$ [13]. Sensing film thickness was assumed negligible.

4) Model Assumptions: ~~The model assumes incompressible~~ Incompressible flow, i.e. $\nabla \cdot \mathbf{u} = 0$, and a no-slip boundary ~~condition~~ conditions were assumed at vessel walls, i.e. $\mathbf{u} = 0$, with initial conditions $\mathbf{u}_0 = \langle 0, 0, 0 \rangle$ m/s and $P_0 = 13.1$ kPa. A no-flux condition is applied at the outer lateral boundaries of the microcirculatory unit since oxygen flux across unit boundaries is considered negligible [13]. The reaction term for oxygen within the capillary is defined as ~~$R_{\text{cap}} = \nabla V \cdot (H C_{\text{Hb}} S_0(P))$~~ $R_c = \nabla V \cdot (H C_{\text{Hb}} S_0(P))$, and at Sp and Ev the oxygen consumption, that is, $R_{\text{sp}} = R_{\text{ev}} = A = 2.23 \times 10^{-3}$ mol/$(m^3 \cdot s)$, with initial concentration ~~$c_0 = 13.3$ kPa~~ $C_0 = 13.3$ kPa [13].

B. FEM Simulation

In experiments reported in [11], the transcutaneous sensor was tested by modulating PaO_2 via i) local occlusion restricting the blood flow and ii) systemic hypoxia reducing the overall oxygen intake as shown in Fig. 2.

We implemented our model in Section III-A using COMSOL Multiphysics. The Grossmann's microcirculatory model was geometrically constructed using a 3D representation with dimensions of 140 × 140 × 240 μm and incorporated a central capillary loop measuring 190 μm in height. Oxygenated blood enters from the arterial end and exits through the venous end of the capillary, with oxygen dissociating from hemoglobin and diffusing across the capillary walls into the surrounding skin layers as shown in Fig. 1.

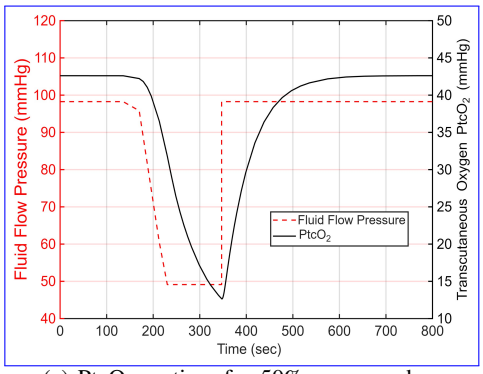

(a) $PtcO_2$ vs time for 50% pressure drop.

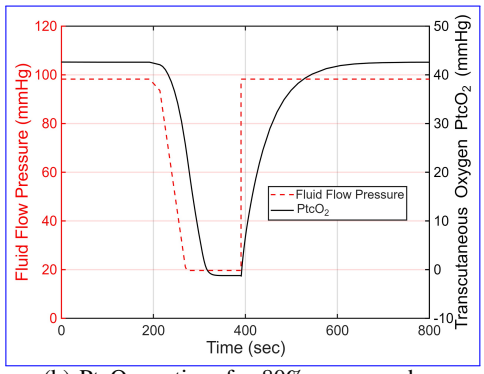

(b) $PtcO_2$ vs time for 80% pressure drop.

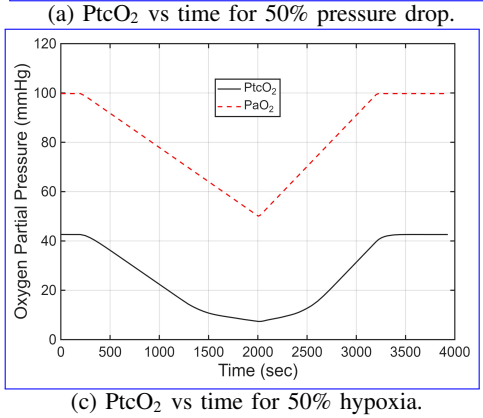

(c) $PtcO_2$ vs time for 50% hypoxia.

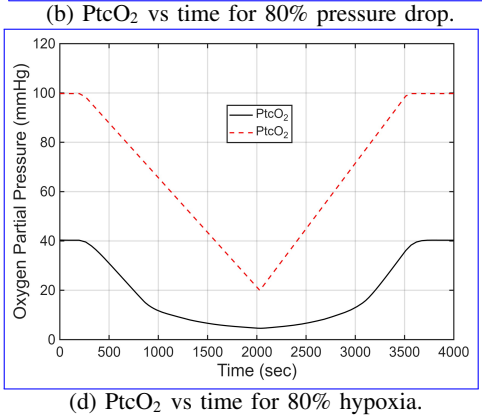

(d) $PtcO_2$ vs time for 80% hypoxia.

Fig. 3: Simulation results showing $PtcO_2$ with respect to time for local occlusion (a-b) and systemic hypoxia (c-d).

The simulation utilized the *Laminar Flow* module to describe hemodynamics within the capillary loop, and the *Transport of Diluted Species* module to model oxygen transport across the skin and into the sensor layer. As COMSOL's transport modules require concentration as the dependent variable, Henry's Law was applied to convert oxygen partial pressure, P, ~~and~~ to concentration, C, using the solubility coefficient, α, as $\alpha P = C$.

Within the *Laminar Flow* module, the capillary was modeled with a no-slip boundary condition and incompressible flow with backflow suppression. In the *Transport of Diluted Species* module, individual transport properties were assigned to each unit component (capillary, stratum papillare (~~Sp~~sp), viable epidermis (~~Ev~~ev), and dead epidermis (~~Ed~~ed)) according to Eqs 1, 3, 2. Reaction boundary conditions were applied inside the capillary to account for hemoglobin-oxygen dissociation, and in the ~~Sp and Ev~~ sp and ev layers for tissue oxygen consumption. No-flux boundaries were enforced at all external surfaces. Once all governing equations and boundary conditions were established, the model was solved using the transient solver.

IV. Results and Discussion

The FEM study was divided into two parts: i) local blood flow occlusion and ii) systemic oxygen inflow variation.

A. Blood Flow Occlusion

As shown in Fig. 2a, applying a blood pressure cuff to upper arm restricts blood flow to the forearm, where the sensor is attached, represented by a drop in the blood pressure. A time dependent study was performed with 50% and 80% linear blood pressure drop and resulting $PtcO_2$ profiles are plotted with respect to time in (Fig. 3a) and (Fig. 3b). After the settling period, a linear occlusion was applied to the blood flow inlet at the capillary for ~~2~~ 3 min and then removed. The simulated occlusions showed an immediate response in $PtcO_2$ levels, reflecting rapid physiological response to decreased perfusion. Notably, the more severe occlusion scenario with 80% pressure drop exhibited a lower $PtcO_2$ during occlusion and reaches this minimum faster, suggesting accelerated ~~oxygen~~ skin oxygen consumption due to limited oxygen availability. Post-occlusion recovery times (around 6 minutes) were consistent across scenarios, emphasizing delayed vascular and metabolic compensatory mechanisms. ~~These resultsclosely align with~~ Unfortunately, there are no reported human data using non-heating $PtcO_2$ ~~recordings~~ measurements for comparison. Moreover, comparison with current $PtcO_2$ devices, with heating elements, is invalid as their measurement will be closer to PaO_2 than our results. However, our recovery time and $PtcO_2$ behavior closely aligned with the experimental results reported in [11].

B. Oxygen Inflow Variation

To replicate the ~~face mask hypoxia study described in~~ hypoxia study [11], a transient simulation was performed using two linear reductions in PaO_2, 50% (Fig. 3c) and 80% (Fig. 3d), modeled ~~as decreased~~ by a decrease in oxygen inflow at the arterial end of the capillary. Following a stabilization period, the oxygen drop was applied for 30 min and was allowed 20-25 min restoration period, based on the hypoxia level, according to [15]. The simulations showed a rapid initial decline in $PtcO_2$ under severe hypoxia, whereas moderate hypoxia resulted in a slower and more gradual decrease, indicating a delayed skin response to less drastic oxygen deprivation. The ~~recovery durations post-hypoxia were found to be identical in both scenarios, suggesting~~

~~intrinsic physiological limits in restoring tissue oxygenation. These results highlight that skin oxygenation dynamics are not instantaneous, hence should be accounted for when converting $PtcO_2$ values to PaO_2.~~ $PtcO_2$ levels gradually returned back to normal following the restoration trend.

Skin and oxygen transport properties vary across individuals due to a range of physiological and environmental factors~~. These variations contribute~~ , leading to differences in $PtcO_2$ measurements. To ~~assess~~ evaluate the impact of this variability, we ~~vary parameters of the model such as the thickness of the live epidermis skin~~ adjusted model parameters based on literature for skin thicknesses [16] and oxygen diffusion ~~coefficient through the blood~~coefficients [17]. The simulation results for $PtcO_2$ are shown with respect to time in Fig. 4a and Fig. 4b for ~~skin thickness~~ different skin thickness factors, k, and in Fig. 4c and Fig. 4d for oxygen diffusion coefficient for both occlusion and hypoxia cases. ~~The increase in~~ Increasing skin thickness led to lower $PtcO_2$, ~~suggesting that it can be used to~~ which can account for personal variabilities in $PtcO_2$ ~~that are shown~~ among men and women. On the other hand, the increase in the diffusion coefficient affected $PtcO_2$ less, but it can be used to account for plasma composition due to ~~various~~ illnesses.

V. Conclusion

Our FEM model accurately simulates the dynamic physiological responses of $PtcO_2$ to both local and systemic changes in PaO_2, demonstrating trends consistent with human experimental data. We also introduce a method for capturing inter-individual variability by adjusting model parameters to reflect personal physiological differences. While still in development, this modeling framework lays the foundation for estimating PaO_2 from $PtcO_2$ measurements combined with personal parameters. This advancement significantly enhances the clinical utility of transcutaneous oxygen sensors and highlights their potential in personalized wearable devices for reliable, continuous respiratory monitoring.

VI. Acknowledgment

This material is based upon work supported by the National Science Foundation under Grant No. OAC-2203827, and by National Institute of Health under Grant No. R01HL172293 and No. R21EB036329. We also thank our collaborator Dr. Ulkuhan Guler and her team in WPI.

References

[1] J. H. Storre, F. S. Magnet, M. Dreher, and W. Windisch, "Transcutaneous monitoring as a replacement for arterial pco2 monitoring during nocturnal non-invasive ventilation," *Respiratory medicine*, vol. 105, no. 1, pp. 143–150, 2011.

[2] A. Fawzy, T. D. Wu, K. Wang, M. L. Robinson, J. Farha, A. Bradke, S. H. Golden, Y. Xu, and B. T. Garibaldi, "Racial and ethnic discrepancy in pulse oximetry and delayed identification of treatment eligibility among patients with covid-19," *JAMA internal medicine*, vol. 182, no. 7, pp. 730–738, 2022.

[3] W. Van Weteringen, T. G. Goos, T. Van Essen, C. Ellenberger, J. Hayoz, R. C. De Jonge, I. K. Reiss, and P. M. Schumacher, "Novel transcutaneous sensor combining optical tcpo 2 and electrochemical tcpco 2 monitoring with reflectance pulse oximetry," *Medical & Biological Engineering & Computing*, vol. 58, pp. 239–247, 2020.

[4] I. Costanzo, D. Sen, J. Adegite, P. M. Rao, and U. Guler, "A noninvasive miniaturized transcutaneous oxygen monitor," *IEEE Transactions on Biomedical Circuits and Systems*, vol. 15, no. 3, pp. 474–485, 2021.

[5] M. M. Kmieć, H. Hou, M. L. Kuppusamy, T. Drews, A. M. Prabhat, S. Petryakov, E. Demidenko, P. E. Schaner, J. C. Buckey, A. Blank, and P. Kuppusamy, "Transcutaneous oxygen measurement in humans using a paramagnetic skin adhesive film," *Magnetic Resonance in Medicine*, vol. 81, pp. 781–794, 2018.

[6] T. Essen, N. Gangaram-Panday, W. Weteringen, T. Goos, I. Reiss, and R. Jonge, "Improving the clinical interpretation of transcutaneous carbon dioxide and oxygen measurements in the neonatal intensive care unit," *Neonatology*, vol. 120, pp. 308–316, 2023.

[7] M. Almatrood, "Grossmann's cross sectional model," https://BioRender.com/k1g5oj9, 2025, created in BioRender.

[8] P. Pape, Z. M. Piosik, C. M. Kristensen, J. Dirks, L. S. Rasmussen, and M. S. Kristensen, "Transcutaneous carbon dioxide monitoring during prolonged apnoea with high-flow nasal oxygen," *Acta Anaesthesiologica Scandinavica*, vol. 67, pp. 649–654, 2023.

[9] A. Cheung, L. Tu, A. Macnab, B. K. Kwon, and B. Shadgan, "Detection of hypoxia by near-infrared spectroscopy and pulse oximetry: a comparative study," *Journal of Biomedical Optics*, vol. 27, 2022.

[10] A. Conway, E. Tipton, W. Liu, Z. J. Conway, K. Soalheira, J. Sutherland, and J. Fingleton, "Accuracy and precision of transcutaneous carbon dioxide monitoring: a systematic review and meta-analysis," *Thorax*, vol. 74, pp. 157–163, 2018.

[11] V. Vakhter, B. Kahraman, G. Bu, F. Foroozan, and U. Guler, "A prototype wearable device for noninvasive monitoring of transcutaneous oxygen," *IEEE Transactions on Biomedical Circuits and Systems*, vol. 17, no. 2, pp. 323–335, 2023.

[12] A. Krogh, "The number and distribution of capillaries in muscles with calculations of the oxygen pressure head necessary for supplying the tissue," *The Journal of physiology*, vol. 52, no. 6, p. 409, 1919.

[13] U. Grossmann, "Simulation of combined transfer of oxygen and heat through the skin using a capillary-loop model," *Mathematical Biosciences*, vol. 61, no. 2, pp. 205–236, 1982.

[14] M. Almatrood, "Human tests scenarios setups," https://BioRender.com/w7zam3o, 2025, created in BioRender.

[15] M. S. Rahman and P. Thomas, "Molecular and biochemical responses of hypoxia exposure in atlantic croaker collected from hypoxic regions in the northern gulf of mexico," *PLoS One*, vol. 12, no. 9, p. e0184341, 2017.

[16] J. Derraik, M. Rademaker, W. Cutfield, T. Pinto, S. Tregurtha, A. Faherty, J. Peart, P. Drury, and P. Hofman, "Effects of age, gender, bmi, and anatomical site on skin thickness in children and adults with diabetes," *Plos One*, vol. 9, p. e86637, 2014.

[17] N. Patel and K. Patel, "Estimation of pulmonary gas exchange in the human respiratory system under normal and abnormal conditions," *Biosciences Biotechnology Research Asia*, vol. 20, no. 1, pp. 255–262, 2023.

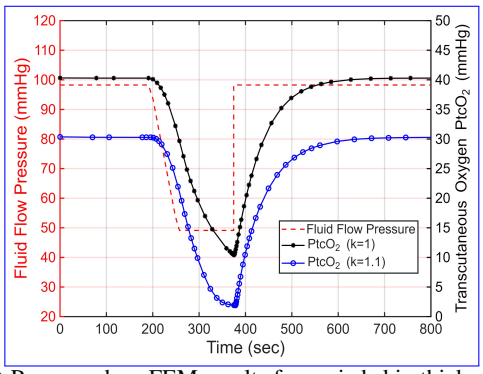

(a) Pressure drop FEM results for varied skin thickness.

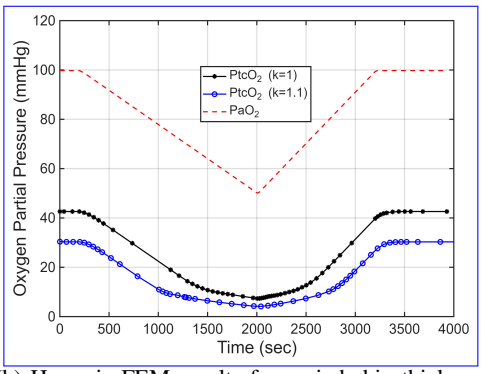

(b) Hypoxia FEM results for varied skin thickness.

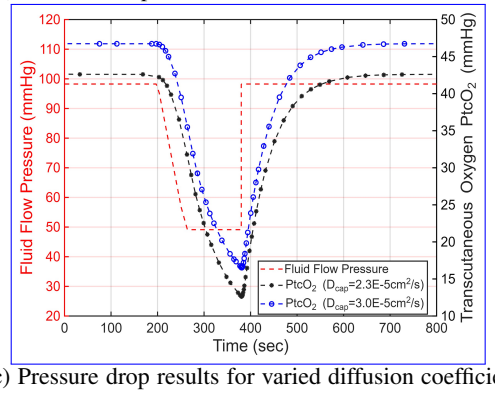

(c) Pressure drop results for varied diffusion coefficient

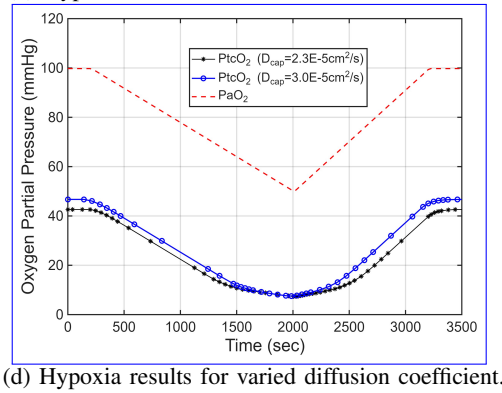

(d) Hypoxia results for varied diffusion coefficient.

Fig. 4: ~~Simulation results for~~ $PtcO_2$ for varying skin thickness (a-b) and diffusion coefficient (c-d) for ~~local~~ occlusion (a-c) and ~~systemic~~ hypoxia (c-d).

1 Reviewer: N72t

Summary: This work introduces a finite element modeling (FEM) framework designed to model the mechanisms which correlates the measurement of arterial oxygen partial pressure (PaO2) via arterial blood gas analysis with transcutaneous oxygen partial pressure (PtcO2) via luminescence based technology. Based on Grossmann's model of oxygen dynamics, the FEM framework agrees with prior human studies for local blood flow occlusion and systemic oxygen inflow variation, demonstrating a proof of concept for use in transcutaneous oxygen monitoring systems.

1.1

Comment 1: Although the model is able to account for generalized variations physiologically, like skin thickness, the paper does not address the effects of varying skin thickness across multiple layers (only observing changes in viable epidermis). Additionally, skin thickness parameters are not readily available in the clinic, and acquiring this information is extremely time consuming and computationally heavy. Further, the values given for the diffusion coefficient in the capillary did not indicate clinical relevance; it would be recommended to observe the minimum, maximum, and median diffusion coefficient to observe the full range of variation in the model. The model also relies on user input to customize the algorithm to suit the patient, implying that diffusion coefficient and skin thickness are available as input parameters; for a real time monitoring device, these parameters could change throughout the day, making clinical translation difficult.

Reply 1: We thank reviewer N72t for the insightful comments and feedback. The manuscript was changed to account for variations in all skin layers and not only the viable epidermis. Specifically, we scaled the thickness of each layer simultaneously using a coefficient, k, to represent overall changes in skin thickness. All the variations are based on the literature review of the human ranges of oxygen diffusion coefficients inside the capillary [1] and skin thickness [2]. The aim of the model is to assess the sensitivity of the $PtcO_2$ levels to varied physiological characteristics. In future work, we plan to develop an algorithm that relates inter- and intra-personal factors to these physiological properties using human subject data. This algorithm will be implemented on the microcontroller of the wearable platform illustrated in [3]. In the final product, users will input only basic parameters (e.g., age, sex, BMI), and the algorithm will estimate corresponding model parameters such as skin thickness. The model will then iteratively solve for PaO_2 based on $PtcO_2$ and the personalized factors.

Changes in manuscript: We updated the results with respect to skin thickness to account for the variation across all skin layers and not only the viable epidermis. We updated Fig. 4 a and b. The references for the values used in variations in skin thicknesses and capillary diffusion coefficients were added to Section IV-B.

1.2

Comment 2: The second to last sentence of Section IV.B. finds that "The recovery durations post-hypoxia were found to be identical in both scenarios, suggesting intrinsic physiological limits in restoring tissue oxygenation". However, the physiological limit in this case would be that the recovery period from 80% hypoxia would elongate; instead, the results of the 80% hypoxia simulation demonstrate that the system recovers at a faster rate, since the time it takes to return to equilibrium is the same as the 50% hypoxia condition. The constraints of mass transport would eventually provide a limit, but this fact is trivial and not a result of the simulation given the fact that no limit was shown. The above blanket statement is unnecessary and does not contribute to the paper meaningfully.

Reply 2: Thank you for your observation. That is correct. Further investigation revealed that complete normalization of PaO_2 usually occurs within approximately 15 to 30 minutes after the removal of the hypoxic stimulus [4]. Based on these findings, a restoration time of 20 and 25 minutes was used for the 50% and 80%, respectively, to account for more reliable recovery time and behavior.

Changes in manuscript: The oxygen inflow variation results were updated to account for a more realistic recovery time from hypoxia. The mentioned statement was modified accordingly, Figure 3 c and d, and Figure 4 b and d were updated.

1.3

Comment 3: There are sections of this paper that had unclear phrasing, convoluted statements, and improper grammar - i.e. under Section II, "Another approach by Grossman build a model based on ..." - that hinders the understanding of the paper. Additionally, the paper's general formatting was poor. For example, under Section III.A, equation 2 utilizes the abbreviations "sp, ev" but does not define this until the last paragraph of Section III.B, forcing the reader to identify the meaning of the abbreviations at a later point. Further, the Figures 3a and 3b were mislabeled, such that the markings should actually show the variation in Fluid Flow Pressure as the red dotted line, while the measured PtcO2 is the black solid line (which would be consistent with Figure 4 and Figure 3c and 3d). Mistakes such as listing "PacO2" were also found, such as in Section III. Finally, the paper fails to adhere to the figure format requested by the conference, specifically in figure text size in the captions of the figures.

Reply 3: We highly appreciate your feedback and thorough comments. The article was proofread and reviewed for any potential typos and/or unclear phrasing.

2 Reviewer: LVyw

Summary: The authors developed a 3D, time-dependent FEM (finite element method) model to simulate how oxygen moves from blood vessels in the skin to a wearable transcutaneous oxygen

($PtcO_2$) sensor. This model includes multiple skin layers and accounts for how oxygen diffuses, flows, and is consumed in the tissue. They simulated two typical situations: local blood flow restriction and reduced oxygen from breathing (hypoxia), and found the model's response closely matches human data. They also explored how differences in skin thickness and oxygen diffusion rates can affect $PtcO_2$ readings across individuals.

2.1

Comment 1: The paper does not mention simulation speed, memory usage, or whether a reduced-order version of the model could run in embedded or real-time settings.

Reply 1: We appreciate this comment and interest in the simulation's specs. We would like to note that this work is a starting point to understand the detailed behavior of PaO_2 and $PtcO_2$, and the sensitivity to different physiological parameters. The next step will be to perform a sweep of parameters over the physiological skin characteristics, derive a relationship between them and inter- and intra- personal factors, and see which factors affect $PtcO_2$ and PaO_2 the most. The final relationship will be used to develop an inverse model to calculate the PaO_2 levels knowing the $PtcO_2$ measurements and the basic personal factors (such as age, gender, BMI) to take into account their role in the physiological skin characteristics.

At the current stage, we do not assess the simulation speed or memory usage as the current model is not intended for direct implementation in a resource-constrained wearable environment. Instead, the derived inverse model will ultimately be embedded in the wearable device. During that phase, we will ensure that the algorithm is optimized for computational efficiency and low memory requirements to enable real-time operation on the wearable platform.

2.2

Comment 2: While the model computes oxygen partial pressure at the skin surface, it does not explain how this would map to luminescent sensor outputs or guide sensor hardware/electronics choices.

Reply 2: Thank you for raising that point. We would like to illustrate that the $PtcO_2$ values found by the model are equal to the ones inside the sensor film. The scope of this work falls around finding the correlation between PaO_2 and $PtcO_2$ only and not focused on the guidance or the hardware of the sensor. The luminescence sensor and hardware aspects were already matured in the literature by our collaborators [3].

2.3

Comment 3: Although the model output follows plausible trends, it is not compared numerically to human data. Metrics such as error rates, delays, or statistical agreement are missing, making it hard to assess accuracy.

Reply 3: We appreciate your comment. We agree that this needs to be addressed. However, due to the novelty of this $PtcO_2$ measuring technique, there are no reported human data to compare

the results directly with. On the other hand, the current clinical $PtcO_2$ monitoring methods use heating elements to increase the diffusion of oxygen through the skin. Comparing our results to these data will not be efficient as their data will be closer to the actual PaO_2. We compare the trends of luminescence lifetime measurements, which are inversely proportional to $PtcO_2$, reported in [3] for an initial assessment of our model for both occlusion and hypoxia cases, and our model's behavior is closely aligned with experimental results reported in [3].

Changes in manuscript: The following text was added to Section IV-A:

"Unfortunately, there are no reported human data using non-heating $PtcO_2$ measurements for comparison. Moreover, comparison with current $PtcO_2$ devices, with heating elements, is invalid as their measurement will be closer to PaO_2 than our results. However, our recovery time and $PtcO_2$ behavior closely aligned with the experimental results reported in [3]."

3 Reviewer: ASZb

Summary: The authors present a finite element modeling (FEM) framework simulating oxygen transport through multilayer skin tissue to characterize the physiological relationship between PaO_2 and $PtcO_2$. The model, validated under local occlusion and systemic hypoxia, is physiologically grounded but omits key optical and physical sensor characteristics, limiting its applicability to real-world transcutaneous oxygen measurements.

3.1

Comment 1: The FEM framework does not include the optical or thermal characteristics of real transcutaneous oxygen sensors (e.g., luminescence excitation/emission, heating effects, sensor-skin interface). This limits the model's ability to predict how $PtcO_2$ would be measured in practice.

Reply 1: Thank you for addressing this point. We would like to note that this work does not deal with the modeling of the hardware of the sensor. Instead, we are dealing with the internal relationship between blood oxygen, PaO_2 and transcutaneous oxygen, $PtcO_2$. The model assumes the absence of heating elements in the sensor, using the proposed sensor by our collaborators [3]. Also, the sensor is flushed with the skin and very well adhered. Hence, the $PtcO_2$ readings from the model reflects the sensor film $PtcO_2$ levels.

3.2

Comment 2: The model specifies initial oxygen partial pressures and applies no-flux boundary conditions at certain skin interfaces, but the manuscript does not provide a detailed physiological rationale for these choices or explore sensitivity to them. Without such justification or analysis, it's unclear how robust the results are to these assumptions.

Reply 2: Thank you for your comment. The model uses a 3D geometry of a skin microcirculatory unit ($140 \times 140 \times 240$ μm) which represents a small part of the human skin with a capillary loop and its corresponding supply volume where multiple adjacent units form a uniform skin tissue.

The model assumes uniform blood flow, oxygen consumption, and diffusion in the skin. Under these conditions, the skin can be represented as identical microcirculatory units (MUs). The collateral boundary surfaces of the microcirculatory units represent surfaces of symmetry for oxygen partial pressure. The boundaries between MUs act as symmetry planes, with no net oxygen diffusion across them, meaning each MU can be considered isolated from its neighbors.

A no-flux boundary condition was applied to the lateral sides of the skin unit to represent the symmetry of the tissue. It was also imposed on the top surface to model the presence of the sensor, assuming it is well adhered to the skin and effectively blocks oxygen exchange with the air. Under this assumption, once equilibrium is reached, the sensing film attains the same oxygen partial pressure as the underlying skin. The sensing film thickness is assumed to be negligible.

Changes in manuscript: We modified Section III-A accordingly to show this explanations.

3.3

Comment 3: The introduction indeed positions the work by contrasting $PtcO_2$ with PaO_2 and SpO_2, but in the actual modeling and simulation, there is no comparative simulation, quantitative analysis, or discussion of SpO_2 or traditional pulse oximetry performance. The focus is entirely on simulating oxygen transport in skin tissue to estimate $PtcO_2$, without modeling light-based SpO_2 measurement or drawing direct comparisons in results.

Reply 3: Thank you for raising this point. The aim of the introduction was to introduce the current methods of monitoring respiratory parameters. SpO_2 was mentioned in the context that, despite its downsides, it provides a non-invasive measurement. The focus shifts later in the introduction to the promising transcutaneous oxygen monitoring methods. Current $PtcO_2$ method still has its drawback due to the use of heating elements. The main goal of this paper is to support the work done by our collaborators [3] by finding a relationship between $PtcO_2$ and PaO_2 to make $PtcO_2$ a more reliable parameter without the use of heating elements or invasive methods.

References

[1] N. Patel and K. Patel, "Estimation of pulmonary gas exchange in the human respiratory system under normal and abnormal conditions," *Biosciences Biotechnology Research Asia*, vol. 20, no. 1, pp. 255–262, 2023.

[2] J. Derraik, M. Rademaker, W. Cutfield, T. Pinto, S. Tregurtha, A. Faherty, J. Peart, P. Drury, and P. Hofman, "Effects of age, gender, bmi, and anatomical site on skin thickness in children and adults with diabetes," *Plos One*, vol. 9, p. e86637, 2014.

[3] V. Vakhter, B. Kahraman, G. Bu, F. Foroozan, and U. Guler, "A prototype wearable device for noninvasive monitoring of transcutaneous oxygen," *IEEE Transactions on Biomedical Circuits and Systems*, vol. 17, no. 2, pp. 323–335, 2023.

[4] M. S. Rahman and P. Thomas, "Molecular and biochemical responses of hypoxia exposure in atlantic croaker collected from hypoxic regions in the northern gulf of mexico," *PLoS One*, vol. 12, no. 9, p. e0184341, 2017.